Solar Energy Conversion and PEM Technology for a Residential Back-up Power System

by

Aaron Biddings

A thesis submitted to the Graduate Faculty of
Auburn University
in partial fulfillment of the
requirements for the Degree of
Master of Science

Auburn, Alabama
May 4, 2013

Keywords: photovoltaic, electrolysis, proton exchange membrane

Approved by

Steven M. Halpin, Chair, Professor, Electrical and Computer Engineering Department
Charles A. Gross, Professor Emeritus, Electrical and Computer Engineering Department
Mark Nelms, Professor and Chair, Electrical and Computer Engineering Department

ABSTRACT

Shown in this work are the characterization, simulation, and implementation of a small-scale back-up power system powered through solar energy conversion. The technical approach utilizes solar arrays with a proton exchange membrane (PEM) electrolyzer and fuel cell. This facilitates the production and storage of electrical energy using hydrogen as a carrier. Proton exchange membrane (PEM) technology was chosen due to its relatively high power density (in comparison with other fuel cell types), its low operating temperature range, and lack of noxious emissions. The setup employs a solar array designed to provide sufficient power to the electrolyzer under varying temperature and lighting conditions. The electrical power is derived directly from the electrochemical energy stored in the hydrogen supply. In this way, the inherent instability and fluctuations in power due to the intermittent nature of solar energy are diminished.

The focus of this study is strictly technical. Monetary cost considerations are beyond the scope of this document.

TABLE OF CONTENTS

Abstract……..……...ii

List of Tables……..……iv

List of Illustrations……..…….v

List of Abbreviations……..……vi

Chapter 1: Introduction……..……..…..1

Chapter 2: Proton Exchange Membrane Fuel Cell….…….....3

Chapter 3: Proton Exchange Membrane Electrolyzer..……10

Chapter 4: Solar Energy Conversion……..……16

Chapter 5: Conclusion……...33

Chapter 6: Further Research……..35

References……...……..36

Appendix A: Determination of Irradiance…….38

Appendix B: Matlab Code For Simulations……...43

LIST OF TABLES

Table A-1. Light Energy, Power, and Irradiance……...40

Table A-2. Error Calculations……41

Table A-3. Adjusted Light Energy, Power, Irradiance, and Percent Error……42

LIST OF ILLUSTRATIONS

Figure 2-1. A) Membrane Electrode Assembly, B) Gas Diffusion Layers, C) Bipolar Plates D) Current Collectors, E) Compression Plates…….…….…...3

Figure 2-2. Activation Loss: 0A-0.2A; Resistive Loss: 0.2A-0.6A; Mass Transport Loss: 0.6A-0.99A……6

Figure 3-1. A) Membrane Electrode Assembly, B) Gas Diffusion Layers, C) Bipolar Plates D) Current Collectors, E) Compression Plates……...10

Figure 3-2. Input Voltage vs. Input Current…..…….……...12

Figure 3-3. Hydrogen Production Rate vs. Input Power.……...13

Figure 4-1. Silicon Solar Cell Cross-section……..17

Figure 4-2. Simple Model of Silicon Solar Cell….……...18

Figure 4-3. Typical Solar Cell I-V Curve……...……...19

Figure 4-4. Effect of Decreasing Shunt Resistance…….……..21

Figure 4-5. Effect of Increasing Series Resistance…….……...22

Figure 4-6. Effect of Increasing Current……..……..24

Figure 4-7. Measured Output Current/Voltage Characteristic……...25

Figure 4-8. Impedance Plot (0.001 Hz ≤ f ≤ 1MHz)…….27

Figure 4-9. Nyquist Plot Representative Circuit……27

Figure 4-10. Effect of Light Intensity on Solar Cell Performance…….……...…29

Figure 4-11. V_{OC} and I_{SC} as Functions of Temperature (°C)…….31

LIST OF ABBREVIATIONS

EIA	Energy Information Administration
H_2O	Water (Dihydrogen Monoxide)
M	Molar Solution (mol/L)
MEA	Membrane Electrode Assembly
PEM	Proton Exchange Membrane

CHAPTER 1: INTRODUCTION

Since the late nineteenth century, when Thomas A. Edison premiered his Pearl Street Station in New York City on September 4, 1882, the generation, transmission, and utilization of electric power has become an indispensible part of everyday living. Much advancement in both equipment and operating practices has been put into effect since those early days. In the United States, the decade of the 1960's was a time of high load growth due to both industrial and commercial expansion. Initially, regulated utilities generated and delivered electric power within localized service areas. Today, the transmission system delivers across states or even regions [1].

In the United States, due to the ubiquity and reliability of the grid, the availability of electric power is generally taken for granted by the public at large. That is, until problems arise and the system fails to deliver. One extreme example of such an outage occurred in 2003 when a wide-area power failure affected millions of Americans across several northeastern states. While outages of this magnitude aren't the norm in the United States, smaller failures do happen occasionally due to various causes ranging from bad weather to aging equipment. In the absence of the main power source, alternate sources may be desired for residential application. Solar arrays used in conjunction with PEM technology may make this a possibility.

Proton exchange membrane (PEM) fuel cells run on hydrogen, which is reported to be the most abundant element on earth. However, it is not usually found in its pure form and must be extracted from a compound. One such well-known compound is none other than H_2O

(water). In the United States, water is supplied directly to most homes. Furthermore, it is unlikely that both the electric power and water supply would fail simultaneously. Therefore, a back-up power system utilizing solar arrays, a PEM electrolyzer, and a PEM fuel cell may be a viable source of intermittent power. The U.S. Energy Information Administration (EIA) reported the average annual electricity consumption for a U.S residential utility customer to be 11,496 kWh in 2010, an average of 958 kWh per month [2]. Thus, the back-up system would need to generate and store enough hydrogen to supply about 32 kWh for daily use.

CHAPTER 2: PROTON EXCHANGE MEMBRANE FUEL CELL

The proton exchange membrane (PEM) fuel cell is an electrochemical cell which functions to combine gaseous hydrogen with oxygen. In the process, only electricity, water, and heat are generated. The basic structure of the PEM fuel cell consists of a membrane electrode assembly (MEA), two gas diffusion layers, two bipolar plates, two current collectors, and two compression plates. See Figure 2-1 for the diagram.

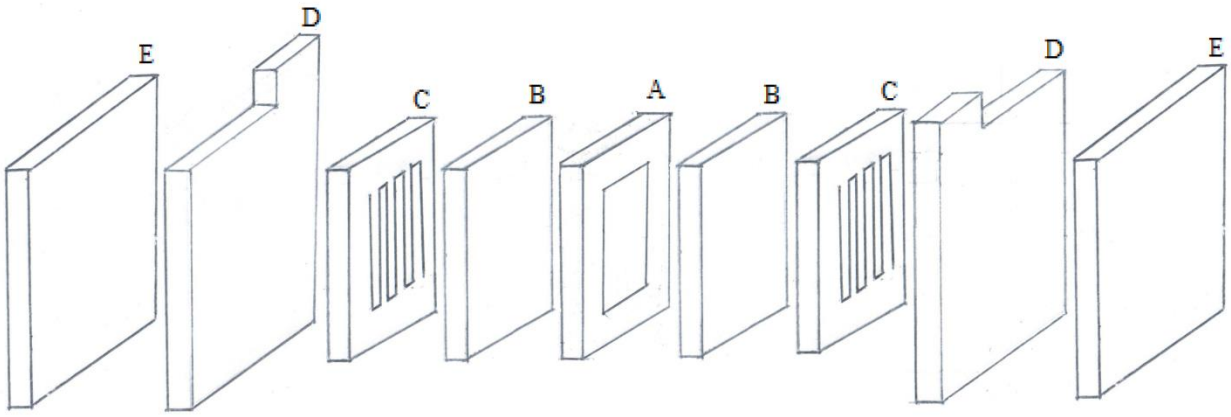

Figure 2-1. A) Membrane Electrode Assembly, B) Gas Diffusion Layers, C) Bipolar Plates D) Current Collectors, E) Compression Plates

The electrochemical reaction that occurs within the fuel cell is described by the equations 2-1 through 2-3 [3].

$$\text{Anode (oxidation): } 2H_2(g) \rightarrow 4H^+(aq) + 4e^- \quad (2\text{-}1)$$

$$\text{Cathode (reduction): } O_2(g) + 4H^+(aq) + 4e^- \rightarrow 2H_2O(l) \quad (2\text{-}2)$$

$$\text{Overall reaction: } 2H_2(g) + O_2(g) \rightarrow 2H_2O(l) \quad (2\text{-}3)$$

The relationship between the fuel cell potential and the concentrations of the products and reactants involved in the electrochemical reaction is described by equations 2-4 and 2-5 [4].

$$Q = \frac{\prod Product\ Activities}{\prod Reactant\ Activities} \tag{2-4}$$

$$E = E° - \frac{R \times T}{n \times F} \times \ln Q \tag{2-5}$$

Equation 2-5 is known as the Nernst equation, where the following definitions apply:

$E =$ Cell potential under nonstandard conditions (V),

$E° =$ Cell potential under standard conditions (V),

$R =$ Ideal gas constant $\left(82.06\ \frac{\text{atm} \times \text{mL}}{\text{mol} \times \text{K}}\right)$,

$T =$ Absolute temperature (K),

$n =$ number of moles of electrons transferred in reaction,

$F =$ Faraday's constant $\left(96485.3\ \frac{\text{C}}{\text{mol}}\right)$, and

$Q =$ Reaction quotient.

Note that in these definitions, standard conditions are P = 1 atm, T = 298.15 K (77 °F), and 1.0 M concentrations.

In order to calculate the fuel cell potential from the redox reaction, it is necessary to obtain the standard potential values for each half-cell reaction within the cell. These may be obtained from the list of standard reduction potentials and are exemplified by equations 2-6 and 2-7 [5].

$$2H^+(aq) + 2e^- \rightarrow H_2(g) \qquad \textbf{(0.0 V)} \tag{2-6}$$

$$O_2(g) + 4H^+(aq) + 4e^- \rightarrow 2H_2O(l) \qquad \textbf{(1.23 V)} \tag{2-7}$$

Each standard reduction potential equation represents a reduction reaction. The cell potential (for non-standard conditions) is found using the concentration values for pure water. Note that non-standard conditions are P = 1 atm, T = 300.4 K (81 °F), $[H^+] = 10^{-7}$ M (for pure water) [6]. So, according to the Nernst equation, the fuel cell output voltage is found as shown in equations 2-8 to 2-12 [4].

$$Q = \frac{1}{(P_{H2})^2 \times P_{O2}} = \frac{1}{1^2 \times 1} \tag{2-8}$$

$$Q = 1 \tag{2-9}$$

$$E_{CELL} = E_C - E_A = (E^\circ{}_C - E^\circ{}_A) - \frac{R \times T}{n \times F} \times \ln Q \tag{2-10}$$

$$E_{CELL} = (1.23\,V - 0.0\,V) - \frac{8.31451 \frac{atm \times mL}{mol \times ^\circ K} \times 300.4\,^\circ K}{4 \times 96485.3 \frac{C}{mol}} \times \ln(1) \tag{2-11}$$

$$E_{CELL} = 1.23\,V \tag{2-12}$$

The positive result of equation 2-12 implies that the reaction is spontaneous. Because this value represents the output, $|E_{CELL}|$ is the theoretical magnitude of the open-circuit voltage (difference between the cathode and anode potentials) of the fuel cell. The magnitude of the measured open-circuit voltage of the fuel cell tested in this work was less than this calculated value.

Three main kinds of losses (also known as overpotentials) affect the operation of a fuel cell: activation loss, resistive loss, and mass transport loss. Each loss causes a reduction in the voltage at the output of the fuel cell. Activation loss is dominant at low current levels. The cause is sluggishness of reactions occurring at the active sites within the fuel cell. Increasing the area of the catalyst may reduce this type of loss. Resistive loss is caused by current flow through

resistive components of the fuel cell such as the membrane, electrodes, contacts, etc. This kind of loss is dominant for moderate current levels. Increasing the hydration of the membrane may reduce this type of loss. Mass transport loss is dominant when current levels are high. The cause of this type of loss is the depletion of reactive species at the electrode surface during heavy loading. More efficient evacuation of reaction product, i.e. water, at the anode may reduce this type of loss. Using a 50 Ω variable resistor as load on the fuel cell under test in this work, a plot of the output voltage versus output current was generated to exemplify these losses. See Figure 2-2.

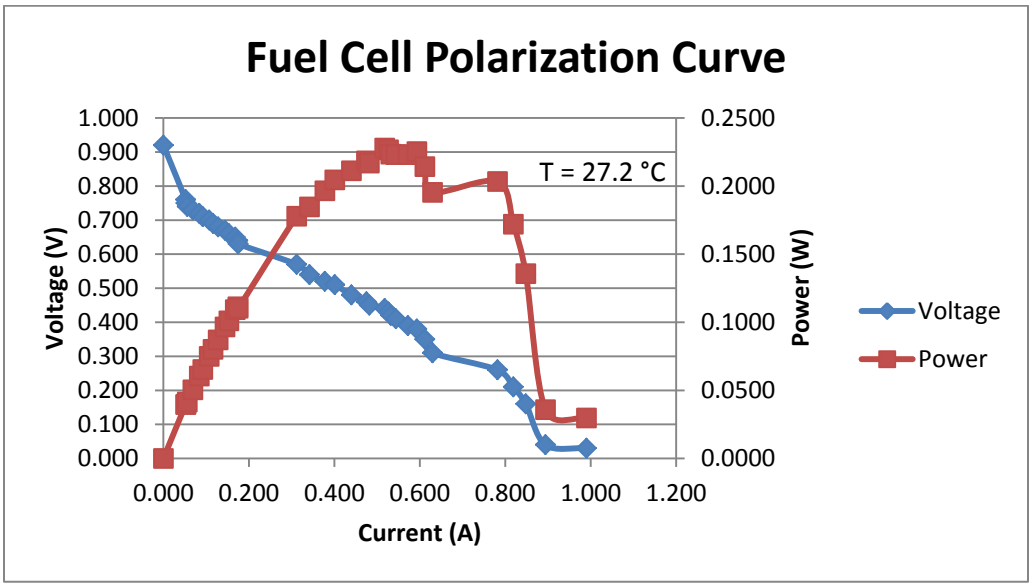

Figure 2-2. Activation Loss: 0A-0.2A; Resistive Loss: 0.2A-0.6A; Mass Transport Loss: 0.6A-0.99A

The ratings of the fuel cell used to produce the polarization curve are: V = 0.6 V, I = 0.4 A, and P = 0.24 W. The membrane electrode assembly of the cell has a measured area of 3.61 cm^2. As observed, a maximum power of 227.9 mW was produced for a voltage of 0.518 V at a current of

0.44 A. At maximum power, the hydrogen fuel consumption rate may be calculated as shown in equations 2-13 to 2-15.

$$R_{H2} = I \times \frac{t_s}{t_m} \times \frac{1}{q} \times \frac{1}{n} \times \frac{1}{N_A} \times M_{H2} \quad (2\text{-}13)$$

$$R_{H2} = 0.44\ A\ \times \frac{60\ s}{1\ min} \times \frac{1\ e^-}{1.602\times10^{-19}\ C} \times \frac{1\ H_2\ atom}{2\ e^-} \times \frac{1\ mol\ H_2}{6.02\times10^{23}\ H_2 atoms} \times \frac{2.01595\ g\ H_2}{1\ mol\ H_2} \quad (2\text{-}14)$$

$$R_{H2} = 2.76 \times 10^{-4}\ \frac{g\ H_2}{min} \quad (2\text{-}15)$$

The following definitions apply in equations 2-13 through 2-15:

$R_{H2} = \mathrm{H_2}$ consumption rate,

$I =$ Current,

$t_s =$ Time in seconds,

$t_m =$ Time in minutes

$q =$ Electron charge $(1.602 \times 10^{-19}\ \mathrm{C})$,

$n =$ Number of electrons per $\mathrm{H_2}$ molecule,

$N_A =$ Avagadro's number $\left(6.02 \times 10^{23}\ \mathrm{mol^{-1}}\right)$, and

$M_{H2} =$ Molar mass of hydrogen molecule, accepted value $\left(2.01595\ \frac{\mathrm{g}}{\mathrm{mol}}\right)$.

The efficiency of this fuel cell at maximum power is calculated in equation 2-16.

$$Eff_{max} = \frac{227.9\ mW \times \frac{1\ \frac{mJ}{s}}{1mW}}{2.76\times10^{-4}\ \frac{g\ H_2}{min} \times \frac{1\ kg}{1000\ g} \times \frac{1\ min}{60\ s} \times \frac{141.86\ MJ}{1\ kg}} \times 100\ \% = 34.9\ \% \quad (2\text{-}16)$$

Maintaining the assumption that the average American household uses about 32 kWh per day when running at full capacity, the fuel cell will need to be scaled up to meet this demand. The rate of daily energy usage, however, will not be constant throughout the day. In order to

simplify the problem, the typical day is broken into 3 intervals: 12am-8am (morning), 8am-4pm (noon), and 4pm-12am (evening). It is likely that most U.S. citizens will sleep during the morning interval, work or attend school during the noon interval, and arrive home to actively use electricity during the evening interval. For each interval, the following assumptions are made:

1) morning energy consumption: 33%,

2) noon energy consumption: 27%, and

3) evening energy consumption: 40%.

The fuel cell's capacity must, therefore, match the greatest load requirement of 40% of daily usage during an 8-hour interval.

$$A_{f\_stack} = A_{FC} \times \frac{E_{house,evening}}{E_{FC,max}} \tag{2-17}$$

$$A_{f\_stack} = 3.61\ cm^2 \times \frac{0.40 \times 32\ kWh}{227.9\ mW \times 8\ hr} = 2.6\ m^2 \tag{2-18}$$

The following definitions apply in equations 2-17 and 2-18:

A_{f_stack} = Total MEA area of fuel cell stack,

A_{FC} = MEA area of fuel cell (under test in this work),

$E_{house,evening}$ = Daily residential energy usage during the evening interval, and

$E_{FC,max}$ = Maximum energy output of fuel cell during evening interval.

Nafion membranes can have a thickness in the range of 127 to 254 microns [7]. The thickness of the fuel cell used in this analysis was measured to be 0.2 cm. Thus, a 13-cell stack with an MEA area of 0.2 m^2 per cell would have minimal space requirements. The average rates of hydrogen consumption by the stack are calculated in equations 2-19 through 2-21.

$$R_{fs\_morning} = \frac{0.33 \times 32\ kWh}{8\ hr} \times \frac{3.6\ MJ}{1\ kWh} \times \frac{1\ kg\ H_2}{141.86\ MJ} \times \frac{1\ hr}{60\ min} = 0.6\ \frac{g\ H_2}{min} \quad (2\text{-}19)$$

$$R_{fs\_noon} = \frac{0.27 \times 32\ kWh}{8\ hr} \times \frac{3.6\ MJ}{1\ kWh} \times \frac{1\ kg\ H_2}{141.86\ MJ} \times \frac{1\ hr}{60\ min} = 0.5\ \frac{g\ H_2}{min} \quad (2\text{-}20)$$

$$R_{fs\_evening} = \frac{0.4 \times 32\ kWh}{8\ hr} \times \frac{3.6\ MJ}{1\ kWh} \times \frac{1\ kg\ H_2}{141.86\ MJ} \times \frac{1\ hr}{60\ min} = 0.7\ \frac{g\ H_2}{min} \quad (2\text{-}21)$$

Moreover, the rate of water consumption necessary to sustain the maximum average demand was found according to equations 2-22 and 2-23.

$$R_{H2O} = 0.7\ \frac{g\ H_2}{min} \times \frac{1\ mol\ H_2}{2.01595\ g\ H_2} \times \frac{1\ mol\ H_2O}{1\ mol\ H_2} \times \frac{18.0166\ g\ H_2O}{1\ mol\ H_2O} \times \frac{1\ gal\ H_2O}{3785\ g\ H_2O} \quad (2\text{-}22)$$

$$R_{H2O} = \frac{0.002\ gal\ H_2O}{1\ min} = 0.1\ \frac{gal}{hr} \quad (2\text{-}23)$$

The total water consumed would amount to less than 2.4 $\frac{\text{gal}}{\text{day}}$. An electrolyzer would need to replenish the supply of hydrogen lost to the fuel cell.

CHAPTER 3: PROTON EXCHANGE MEMBRANE ELECTROLYZER

The proton exchange membrane (PEM) electrolyzer is an electrochemical cell which functions to separate water into its constituent elements using electrolysis. The basic structure is the same as that of a PEM fuel cell: a membrane electrode assembly (MEA), two gas diffusion layers, two bipolar plates, two current collectors, and two compression plates. See Figure 3-1 for the diagram.

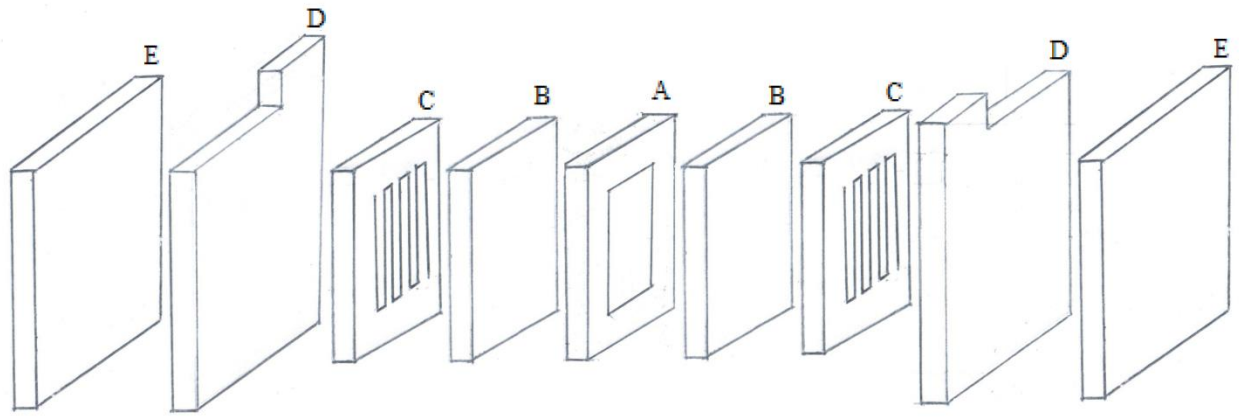

Figure 3-1. A) Membrane Electrode Assembly, B) Gas Diffusion Layers, C) Bipolar Plates D) Current Collectors, E) Compression Plates

Equations 3-1 to 3-3 govern the reactions within the electrolyzer cell [3].

$$\text{Cathode (reduction): } 4H^+(aq) + 4e^- \rightarrow 2H_2(g) \quad (3\text{-}1)$$

$$\text{Anode (oxidation): } 2H_2O(l) \rightarrow O_2(g) + 4H^+(aq) + 4e^- \quad (3\text{-}2)$$

$$\text{Overall reaction: } 2H_2O(l) \rightarrow 2H_2(g) + O_2(g) \quad (3\text{-}3)$$

The electrolyzer cell potential is calculated in a way similar to that of the fuel cell. From the list of standard reduction potentials, the standard potentials for each half cell reaction are again shown in equations 3-4 and 3-5 [5].

$$2H^+(aq) + 2e^- \rightarrow H_2(g) \qquad \textbf{(0.0 V)} \tag{3-4}$$

$$O_2(g) + 4H^+(aq) + 4e^- \rightarrow 2H_2O(l) \qquad \textbf{(1.23 V)} \tag{3-5}$$

The cell potential for the electrolyzer cell is found using the Nernst equation [4].

$$Q = \frac{(P_{H2})^2 \times P_{O2}}{1} = \frac{(1)^2 \times 1}{1} = 1 \tag{3-6}$$

$$E_{CELL} = E_C - E_A = (E^\circ{}_C - E^\circ{}_A) - \frac{R \times T}{n \times F} \times \ln Q \tag{3-7}$$

$$E_{CELL} = (-1.23\ V - 0.0\ V) - \frac{8.31451 \frac{atm \times mL}{mol \times ^\circ K} \times 296.5\ ^\circ K}{2 \times 96485.3 \frac{C}{mol}} \times \ln(1) \tag{3-8}$$

$$E_{CELL} = -1.23\ V \tag{3-9}$$

The negative sign of the result implies that the reaction is not spontaneous. Because this result is the value of the input voltage to the electrolyzer cell, $|E_{CELL}|$ represents the theoretical magnitude of the minimum applied voltage (difference between cathode and anode potentials) for which the electrolyzer will begin to separate hydrogen from the water molecules for non-standard conditions, i.e P = 1 atm, T = 296.5 K (74 °F), and $[H^+] = 10^{-7}$ M.

Whereas the MEA was measured to be 6.25 cm^2, the specifications provided by the manufacturer for the electrolyzer used in this analysis are the following [8]:

1) 1.7 V to 3.0 V (input), and

2) 1 A current @ 2.0 V (input).

Using the Tenma® Laboratory DC power supply 72-2080, an input voltage/current plot was produced as shown in Figure 3-2 for 100 mA increments in the range from 0.1 A to 1.2 A.

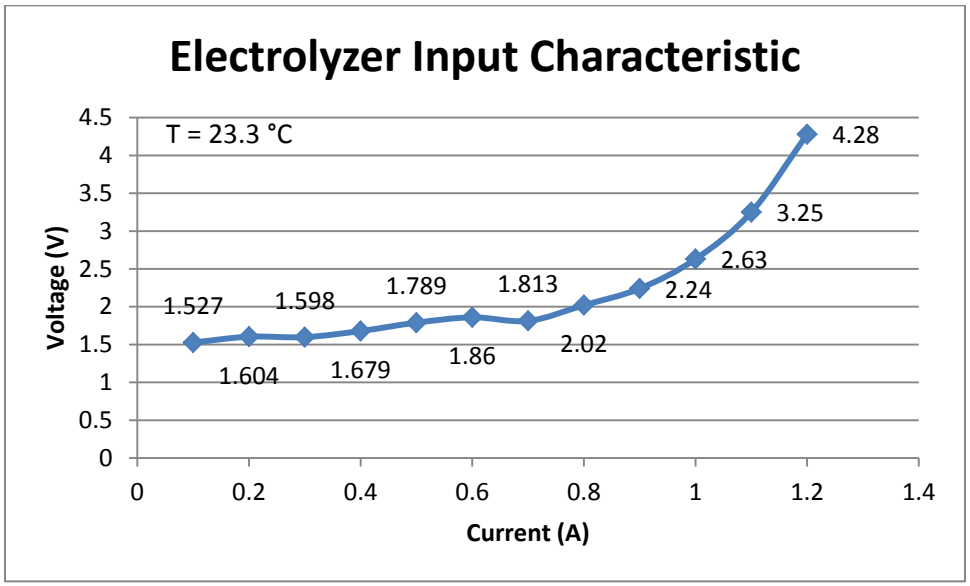

Figure 3-2. Input Voltage vs. Input Current

Again using the DC power supply, along with a graduated cylinder and a timer, the hydrogen production rate was plotted as a function of the input power. The current served as the controlled variable in increments of 100 mA from 0.1 A to 1.2 A. See Figure 3-3 for the plot.

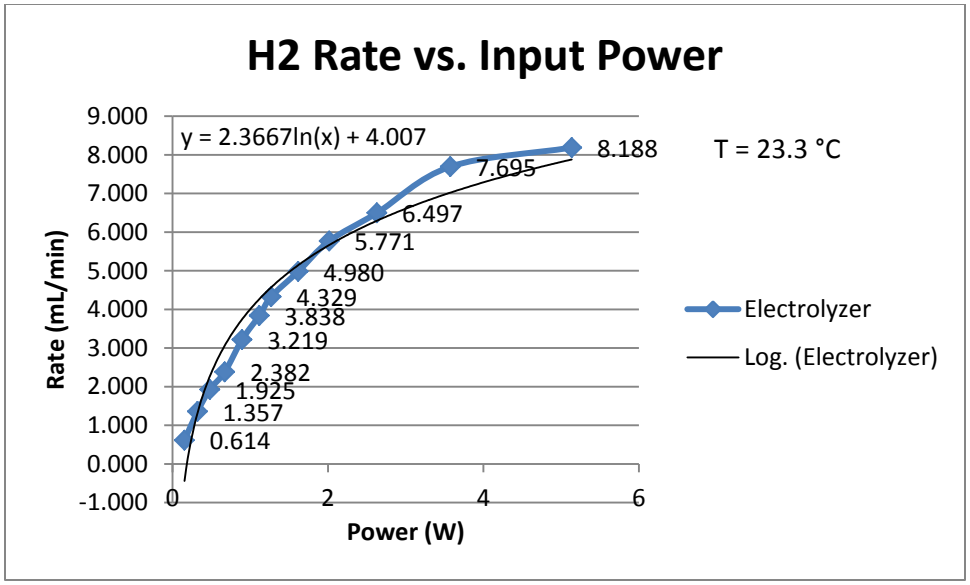

Figure 3-3. Hydrogen Production Rate vs. Input Power

As is visible from Figure 3-3, the hydrogen production rate increased at a diminishing pace as the input power increased. This phenomenon is most likely due to mass transport limitations of the reactive species that become more dominant as the current increases. Using Excel curve fitting functionality, the input to output relationship is shown to closely approximate a logarithmic function. (Current levels above 1.2 A were avoided due to an issue with overheating and destruction of the MEA gasket.)

According to calculations in Chapter 2, the postulated PEM fuel cell stack would consume hydrogen at a maximum average rate of 0.7 $\frac{\text{g H}_2}{\text{min}}$ during the evening interval. The electrolyzer cell under test in this work (MEA of 6.25 cm^2) produced hydrogen at a rate of 8.188 $\frac{\text{ml H}_2}{\text{min}}$ at 5.136 W for a current of 1.2 A. By the ideal gas law [9], the hydrogen production rate by mass at 23.3 °C (74 °F) was approximated in equations 3-10 and 3-11.

$$n = \frac{P \times V}{R \times T} = \frac{1\ atm \times 8.188\ mL}{82.06 \frac{atm \times mL}{mol \times °K} \times 296.5\ °K} = 3.37 \times 10^{-4}\ mol \quad (3\text{-}10)$$

$$R_{elec} = 3.37 \times 10^{-4} \frac{mol\ H_2}{min} \times \frac{2.01595\ g\ H_2}{1\ mol\ H_2} = 6.78 \times 10^{-4}\ \frac{g\ H_2}{min} \quad (3\text{-}11)$$

The overall efficiency of the electrolyzer cell was calculated in equations 3-12 and 3-13.

$$P_{OUT} = 8.188\ \frac{ml\ H_2}{min} \times \frac{1\ min}{60\ s} \times 0.08286\ \frac{kg\ H_2}{m^3\ H_2}\Big|_{T=23.3\ °C} \times \frac{1\ m^3\ H_2}{1 \times 10^6\ ml\ H_2} \times \frac{141.86\ MJ}{1\ kg\ H_2} = 1.604\ W \quad (3\text{-}12)$$

$$eff = 100\% \times \frac{P_{OUT}}{P_{IN}}\Big|_{I=1.2\ A} = 100\% \times \frac{1.604\ W}{5.136\ W}\Big|_{I=1.2\ A} = 31.23\% \quad (3\text{-}13)$$

The electrolyzer would be required to replenish the hydrogen supply used by the fuel cell. Therefore, the amount of hydrogen lost is needed to calculate the size of the electrolyzer stack.

Because the system will derive its power from solar energy conversion, the noon interval would be the optimal time for hydrogen production. Starting with a full tank of hydrogen, the worst case scenario would be a total main power failure beginning a 4pm and lasting for 24 hours. The amount of hydrogen consumed by the fuel cell during the evening and morning intervals (while the electrolyzer is powered down) is calculated in equations 3-14 and 3-15.

$$m_{H2} = \left(R_{fs\_morning} + R_{fs\_evening}\right) \times t \quad (3\text{-}14)$$

$$m_{H2} = \left(0.6\ \frac{g\ H_2}{min} + 0.7\ \frac{g\ H_2}{min}\right) \times \left(\frac{60\ min}{1\ hr}\right) \times 8\ hr = 624\ g\ H_2 \quad (3\text{-}15)$$

The electrolyzer will need to replenish this amount in addition to keeping up with the noon energy demand. The necessary rate of hydrogen production was found according to equation 3-16.

$$R_{e\_stack} = \frac{m_{H2}}{t_{noon}} + R_{fs\_noon} = \frac{624\ g\ H_2}{8\ hr} \times \frac{1\ hr}{60\ min} + 0.5\ \frac{g\ H_2}{min} = 1.8\ \frac{g\ H_2}{min} \quad (3\text{-}16)$$

Scaling up the electrolyzer to match this hydrogen production rate gives a membrane electrode assembly with an area as found by equation 3-17.

$$A_{e\_stack} = A_{elec} \times \frac{R_{e\_stack}}{R_{elec}} = 6.25\ cm^2 \times \frac{1.8 \frac{g\ H_2}{min}}{6.78 \times 10^{-4} \frac{g\ H_2}{min}} = 1.7\ m^2 \qquad (3\text{-}17)$$

The following definitions apply in equation 3-17:

$A_{e\_stack} =$ Area of electrolyzer stack MEA,

$A_{elec} =$ Area of electrolyzer cell MEA (under test in this work),

$R_{e\_stack} =$ Rate of electrolyzer stack hydrogen production, and

$R_{elec} =$ Rate of electrolyzer cell hydrogen production.

Similar to the fuel cell, the thickness of the electrolyzer's membrane is small. The thickness of the electrolyzer cell used in this analysis was measured to be 0.3 cm. So, a nine-cell electrolyzer stack with an MEA area of 0.2 m^2 per cell is sufficient to meet the specified mass flow rate. Also, the space requirements are not significant.

Thus, the daily energy demand for the electrolyzer stack is calculated in equations 3-18 and 3-19.

$$E^{in}_{e\_stack} = 1.8\ \frac{g\ H_2}{min} \times \frac{60\ min}{1\ hr} \times \frac{1\ kg\ H_2}{1000\ g\ H_2} \times \frac{141.86\ MJ}{1\ kg\ H_2} \times \frac{1\ kWh}{3.6\ MJ} \times 8\ hr \qquad (3\text{-}18)$$

$$E^{in}_{e\_stack} = 34.1\ kWh \qquad (3\text{-}19)$$

If a solar array is incorporated into the system design, it must match the energy need of this electrolyzer stack.

CHAPTER 4: SOLAR ENERGY CONVERSION

A solar array is a photovoltaic device which consists of a collection of solar cells arranged in a combination of rows and columns. The solar cell is the basic unit of photovoltaic energy conversion and is manufactured from semiconductor materials. There are three general categories of photovoltaic cells currently on the market. They are the monocrystalline, polycrystalline, and thin film (or amorphous) cells [10]. The monocrystalline solar cell is cut from a continuous crystal of silicon. While is has the greatest efficiency, it is also the most expensive type of solar cell. The polycrystalline solar cell is cut from a block of silicon which had been previously melted and poured into a mold. As the silicon cools, many crystals are formed throughout its bulk. Polycrystalline solar cells are slightly less efficient than the monocrystalline variety. Finally, the thin film (or amorphous) solar cell contains no crystals and is made by depositing a microscopically thin layer of silicon on a backing material such as some other metal or glass. For the purpose of this analysis a polycrystalline silicon solar cell was utilized.

The structure of a solar cell is such that it consists of several layers: the front contacts, the antireflection coating, the n-substrate material, the p-substrate material, and the rear contacts. See Figure 4-1 for the solar cell diagram.

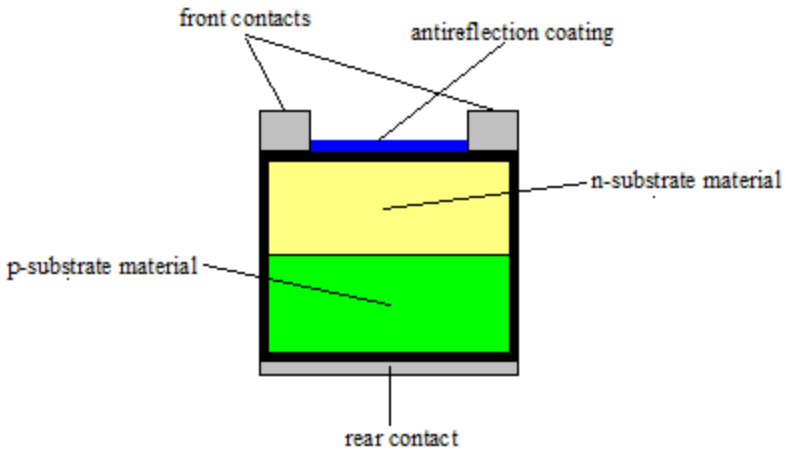

Figure 4-1. Silicon Solar Cell Cross-section (Not to scale)

When a photon of sufficient energy strikes the cell it gets absorbed. In the process, the photon transfers its energy to the silicon lattice creating an electron/hole pair. The electron is simultaneously raised from the valence band to the conduction band where it is capable of doing electrical work, e.g. flowing though an external circuit.

The simplest model of a solar cell takes into account the effects of the p-n junction, light-generated current, series resistance, and internal shunt resistance. The simple solar cell model circuit is shown in Figure 4-2.

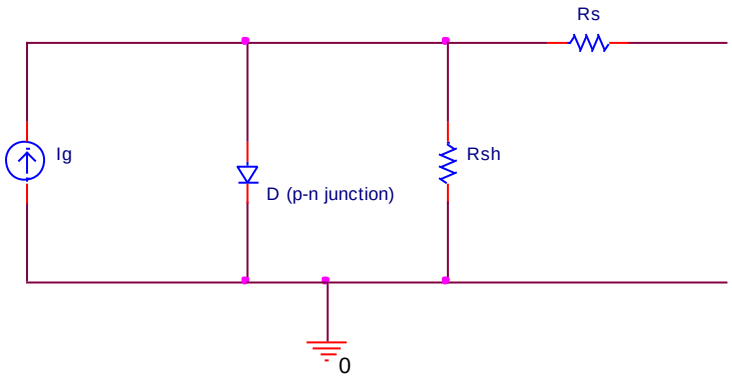

Figure 4-2. Simple Model of Silicon Solar Cell [11]

In the model, the light generated current is represented by the independent current source; the diode represents the p-n junction; and the series and shunt resistances are represented by the resistors R_S and R_{SH}, respectively.

Analysis of a solar cell is usually done in terms of its output current/voltage relationship. Three methods used differ in their results due to the internal resistance of the solar cell. These three characteristics are the following: photovoltaic output characteristic, diode forward characteristic, and the p-n junction characteristic [12]. The first method employs a fixed illumination (usually) of known intensity while varying a load resistance between short-circuit and open-circuit. Voltage and current measurements are recorded for each resistor setting. The second method uses no illumination, but instead applies a variable source to the output terminals of the cell. The current is, therefore, measured and plotted against the voltage as it is varied over a certain range. The third method varies the light intensity while measurements of the open-circuit voltage and short-circuit current are taken for each light setting. Because the conditions

of the photovoltaic analysis are similar to those of normal operation, this type of analysis is the focal point of this study.

The p-n junction of a solar cell determines the output current/voltage relationship. However, the internal resistance can cause significant effects. A good quality cell has a large shunt resistance and a small series resistance and produces an I-V curve similar to that shown in Figure 4-3. This is an example of a typical photovoltaic output characteristic curve.

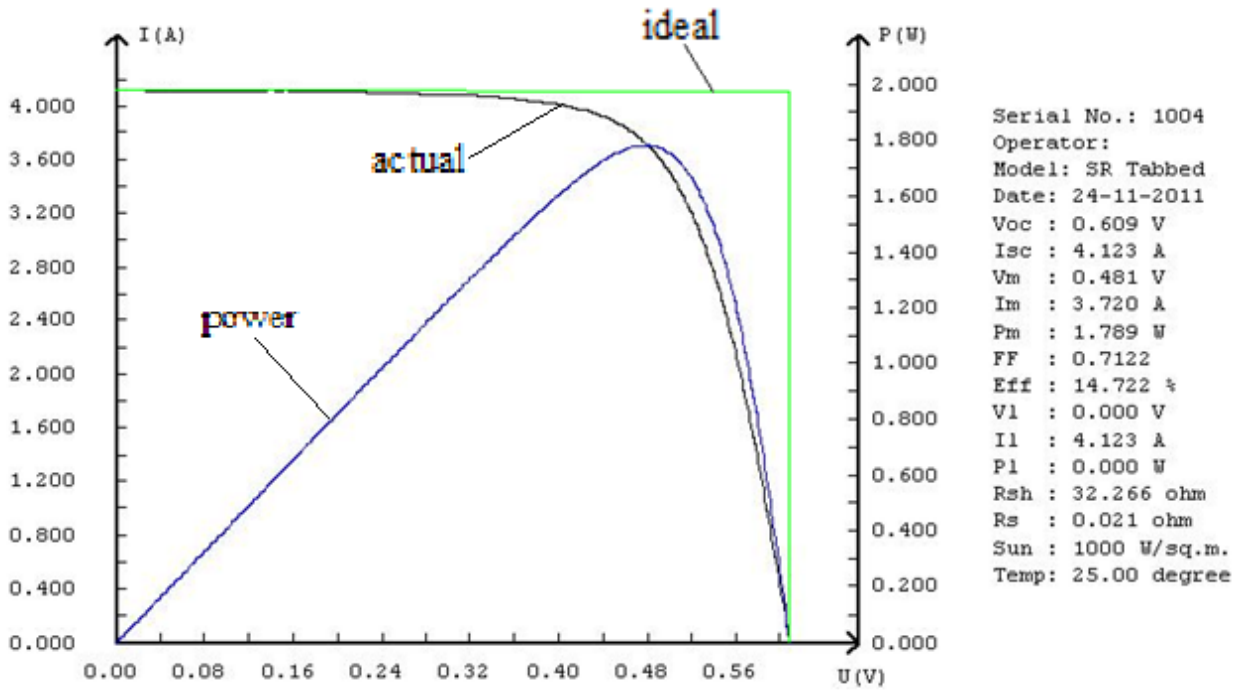

Figure 4-3. Typical Solar Cell I-V Curve (Source: Everbright Solar, Inc.)

In order to understand how the series and shunt resistances affect the output characteristic, MATLAB® simulations were performed in which one quantity was held constant while the other was varied. To facilitate the analysis, the circuit equation 4-1 was derived from Figure 4-2 (incorporating a load resistance).

$$I_G = I_S\left(e^{\frac{q*V_D}{\eta*k*T}} - 1\right) + \frac{V_D}{R_{SH}} + \frac{V_D}{R_S + R_L} \quad (4\text{-}1)$$

The following definitions apply in equation 4-1:

$I_G = \text{Internal Light} - \text{Generated Current (A)},$

$I_S = \text{p} - \text{n Junction Saturation Current (A)},$

$q = \text{Electron Charge } (1.602 \times 10^{-19}\ \text{C}),$

$V_D = \text{p} - \text{n Junction Voltage (V)},$

$\eta = \text{Emission Coefficient},$

$k = \text{Boltzmann Constant } \left(1.380658 \times 10^{-23}\ \frac{\text{J}}{\text{K}}\right),$

$T = \text{Absolute Temperature (K)},$

$R_{SH} = \text{Shunt Resistance } (\Omega),$

$R_S = \text{Series Resistance } (\Omega), \text{and}$

$R_L = \text{Load Resistance } (\Omega).$

In the first simulation, the series resistance was held constant (R_S = 0.167 Ω). (This value represents the actual series resistance of the cell under test in this work.) Four separate plots were generated for distinct values of shunt resistance while the load resistance was varied from R_L = 0 Ω to 50 Ω in each case. The values chosen for the shunt resistance represent the measured resistance of the solar cell under test in this work and three submultiples of the same. See Figure 4-4 for the plots of load current versus the load voltage.

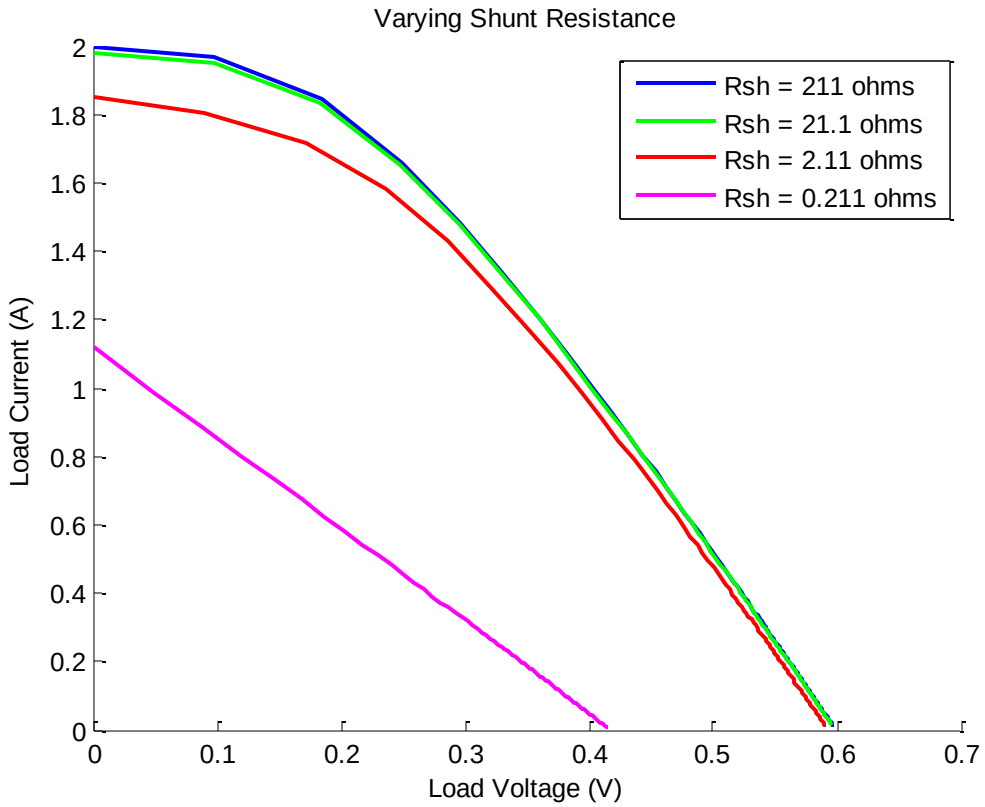

Figure 4-4. Effect of Decreasing Shunt Resistance

The initial effect of reducing the shunt resistance is that both the short-circuit current and open-circuit voltage are slightly diminished. However, upon further decrease, the shunt resistance begins to dominate the p-n junction; the exponential curve eventually become linear and appears as purely resistive.

In the second simulation, the shunt resistance was held constant (R_{SH} = 211 Ω). (This value represents the actual shunt resistance of the cell under test in this work.) Four separate plots were generated for distinct values of series resistance while the load resistance was varied from R_L = 0 Ω to 50 Ω in each case. The values chosen for the series resistance represent the

measured resistance of the solar cell under test in this work and three integer multiples of the same. See Figure 4-5 for the plots of load current versus the load voltage.

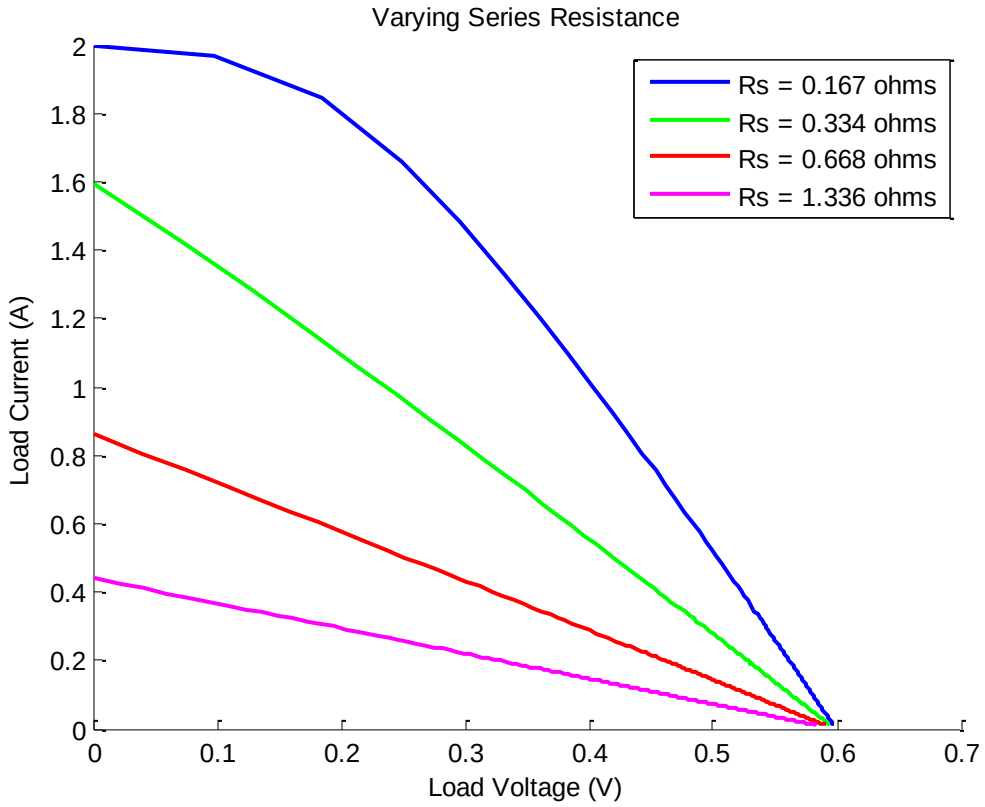

Figure 4-5. Effect of Increasing Series Resistance

Increasing the series resistance produces a similar but more dramatic reduction in the short-circuit current as compared to the incremental reduction in the shunt resistance. Also, the series resistance begins to dominate the output characteristic producing a straight line. However, unlike the case with shunt resistance, the open-circuit voltage remains unaffected. Thus, the combination of a large series resistance and a small shunt resistance works to lower both the

open-circuit voltage and short-circuit current from their ideal. In solar cells of lower quality, the output characteristic begins to look more resistive.

One additional note on the output current/voltage relationship of a solar cell is that for given shunt and series resistances, large light-generated current may also produce linearization of the output characteristic due to the fact that much of this current effectively "bypasses" the p-n junction but passes through the resistances. Holding the series resistance constant (R_S = 0.167 Ω) and the shunt resistance constant (R_{SH} = 211 Ω), six plots were produced for distinct values of light-generated current while the load resistance was varied from R_L = 0 Ω to 50 Ω in each case. The values chosen for the light generated current represent the rated current of the solar cell under test in this work and submultiples of the same. In Figure 4-6 is shown plots of load current versus load voltage.

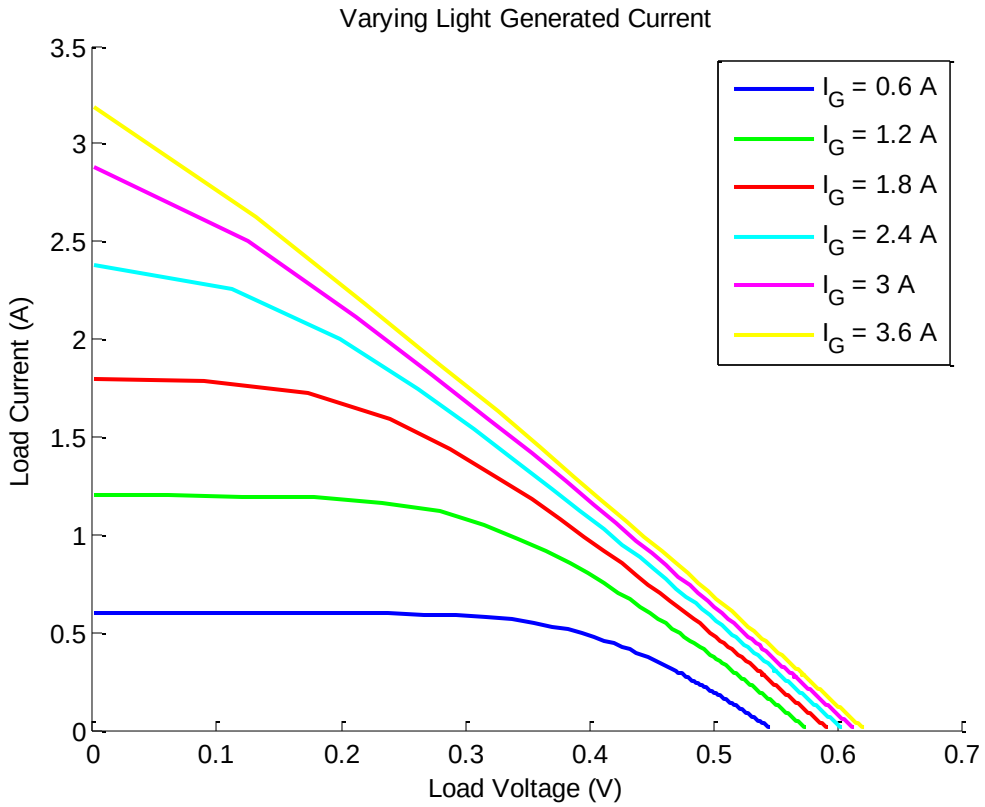

Figure 4-6. Effect of Increasing Current

Now that the ground work has been established for properly analyzing the photovoltaic output characteristic of a solar cell, the actual measurements may be interjected. The ratings of the cell under test were 1.8 W, 0.5 V, and 3.6 A. Using a 50 Ω variable resistor as load and a 1500 lumens/100 W bulb (at a distance of 30.48 cm) for constant illumination, the solar cell output characteristic was plotted. The outcome of the analysis is shown in Figure 4-7.

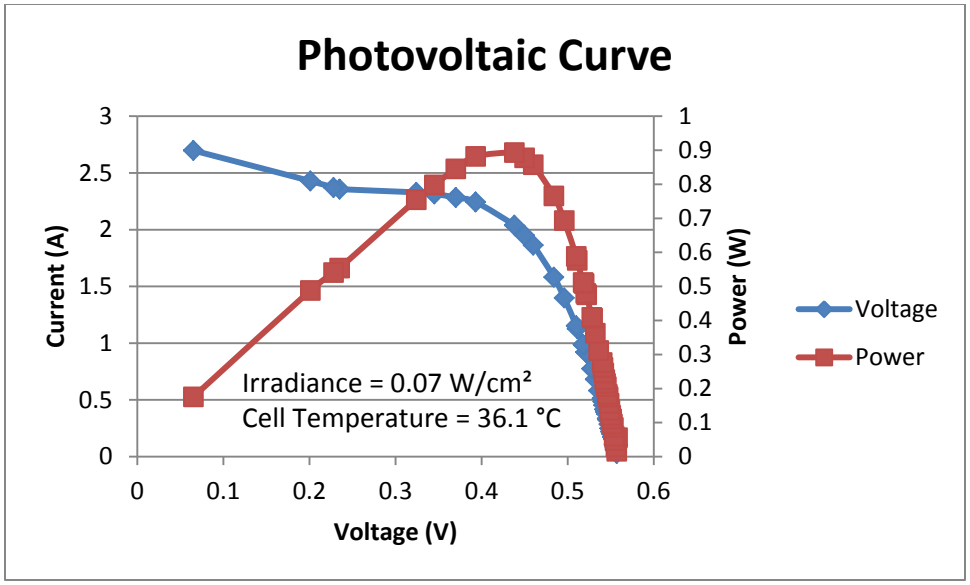

Figure 4-7. Measured Output Current/Voltage Characteristic

The good curvature of the current/voltage plot implies that neither the series nor shunt resistances dominate the p-n junction. It should be noted that the non-zero resistance of the tabbing wire used to short the solar cell terminals prevented the output voltage from reaching zero.

The irradiance on the cell for the light source used was found to be 0.07 W/cm^2. (See Appendix A for an explanation of how to determine irradiance.) With a solar cell surface area of 116.13 cm^2, the incident power was calculated to be 8.89 W. The maximum cell output power of 0.893 W yielded an efficiency shown by equation 4-2.

$$eff = 100\,\% \times \frac{P_{OUT}}{P_{IN}} = 100\,\% \times \frac{0.893\,W}{8.89\,W} = 10.04\,\% \qquad (4\text{-}2)$$

The series resistance can usually be estimated from the slope of the curve at the open circuit point; the shunt resistance can be estimated from the slope at the short circuit point. However, a more accurate method for acquiring both resistances entailed using AC analysis. This analysis involved application of a sinusoidal voltage source of constant magnitude to the solar cell. The frequency of the source was varied over a range of values; the resistance and reactance of the cell were simultaneously measured for each frequency. Taken together, the resistance and reactance represent the output impedance of the solar cell. (Given a zero resistance value, a positive reactance value represents pure inductance; a negative reactance value represents pure capacitance. A zero reactance value represents pure resistance. All other numerical combinations signify some interconnection of resistance, capacitance and/or inductance.) From the measured resistance and reactance values a Nyquist plot of the solar cell's output impedance was subsequently generated. This plot is reproduced here in Figure 4-8.

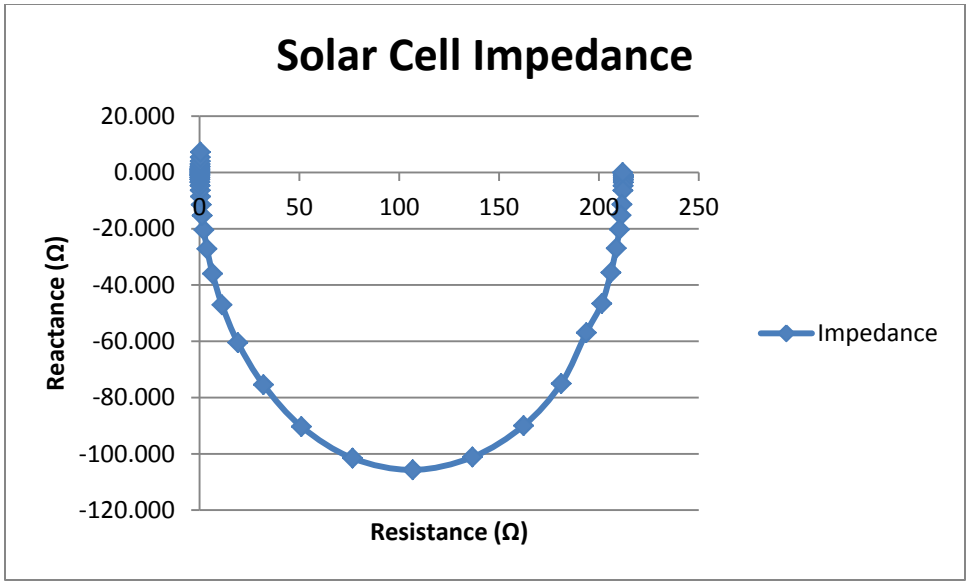

Figure 4-8. Impedance Plot (0.001 Hz ≤ f ≤ 1MHz)

The Nyquist plot of the solar cell impedance was created for a frequency range of 0.001 Hz to 1 MHz. Observance of the plot shows that there were two frequencies for which the reactance was negligible. At each of these frequencies, the solar cell output impedance appeared purely resistive to a good approximation. (Resistance and reactance measurements were simultaneously captured using the Solartron Instruments SI 1260 Impedance/Gain-Phase Analyzer with the SI 12601 component test module.) Figure 4-8 is representative of an R-R/C combination. See Figure 4-9 for the circuit.

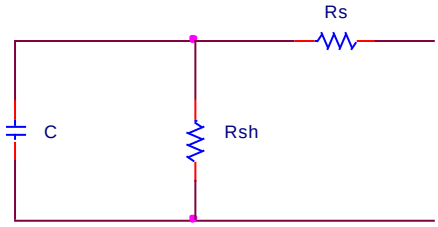

Figure 4-9. Nyquist Plot Representative Circuit

To find the resistances, the circuit equation was derived for Figure 4-9. See equations 4-3 to 4-7 for the derivation.

$$\boldsymbol{Z} = R_S + \frac{1}{\frac{1}{R_{SH}} + \boldsymbol{j}\omega C} = R_S + \frac{R_{SH}}{1 + \boldsymbol{j}\omega C R_{SH}} \tag{4-3}$$

$$\boldsymbol{Z} = \frac{R_S + R_{SH} + \boldsymbol{j}\omega C(R_S \times R_{SH})}{1 + \boldsymbol{j}\omega C R_{SH}} \tag{4-4}$$

$$Z = \frac{\sqrt{(R_S + R_{SH})^2 + \left(\omega C(R_S \times R_{SH})\right)^2}}{\sqrt{1 + (\omega C R_{SH})^2}} \tag{4-5}$$

$$Z|_{\omega \to \infty} = R_S \tag{4-6}$$

$$Z|_{\omega \to 0} = R_S + R_{SH} \tag{4-7}$$

At a frequency of 96,813.02 Hz the measured reactance was at its smallest value and the corresponding impedance was measured to be 0.167 Ω. At the opposite end of the spectrum, for a frequency of 7.71 mHz, the measured reactance was again at its smallest value; the corresponding impedance was measured to be 211.74 Ω. Thus, the series and shunt resistances were found in equations 4-8 and 4-9.

$$R_S = Z|_{\omega = 608294 \frac{rad}{s}} = 0.167\ \Omega \tag{4-8}$$

$$R_{SH} = Z|_{\omega = 0.048 \frac{rad}{s}} - R_S = 211.74\ \Omega - 0.167\ \Omega = 211.573\ \Omega \tag{4-9}$$

The daily light level varies between $0\,\frac{\mathrm{W}}{\mathrm{cm}^2}$ before sunrise/after sunset and $0.1\,\frac{\mathrm{W}}{\mathrm{cm}^2}$ (average value) at noon. Luminous intensity has a considerable effect on the performance of a solar cell. The short-circuit current is directly proportional to the luminous intensity. From equation 4-1, for negligible series ($R_S = 0$) and shunt ($R_{SH} = \infty$) resistances, the open-circuit

voltage has a logarithmic dependence on light intensity (through the short circuit current) according to equation 4-10.

$$V_{OC} = \frac{\eta kT}{q} \times \ln \frac{I_{SC}}{I_S}\Big|_{I_{SC}=I_G} \qquad (4\text{-}10)$$

In Figure 4-10 is shown the effect of light level on both the open-circuit voltage and the short-circuit current for the solar cell under test.

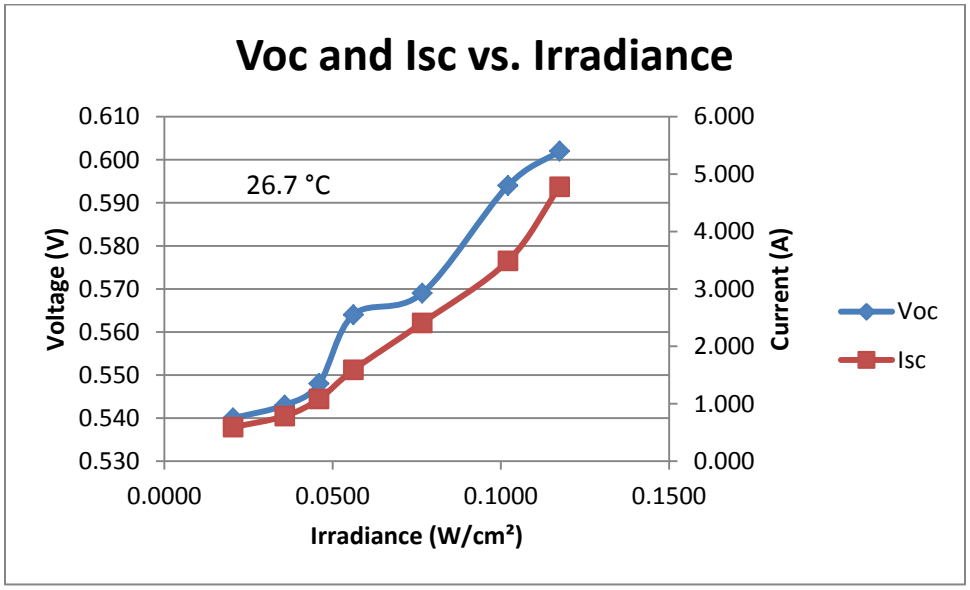

Figure 4-10. Effect of Light Intensity on Solar Cell Performance

A cursory evaluation of Figure 4-10 shows that the short-circuit current increases linearly as luminous intensity rises. Additionally, the open-circuit voltage continues to increase for higher light intensity levels. (When loaded, the shunt resistance effect becomes dominant at low current levels; the series resistance effect becomes dominant at high current levels.)

Changes in temperature will adversely affect the output power of a solar cell. Increasing temperature reduces the band gap of a semiconductor which effectively increases the energy of electrons within the material. Therefore, less energy is necessary to break the bonds and raise those electrons from the valence band to the conduction band. Theoretically, this means that as the temperature rises, the short-circuit current increases; but the open-circuit voltage is reduced. In practice, changes in the internal resistance that occur with temperature may also produce visible effects in the output. According to the simplified p-n junction (diode) equation [13]:

$$V_{OC} = \frac{\eta kT}{q} \times \ln \frac{I_G}{I_S}.$$

The open-circuit voltage is directly proportional to the temperature. However, it is also dependent upon the saturation current I_S which approximately doubles for every 10 °C rise in temperature [14]. In Figure 4-11 is shown the measurement of both the open-circuit voltage and short-circuit current as functions of temperature.

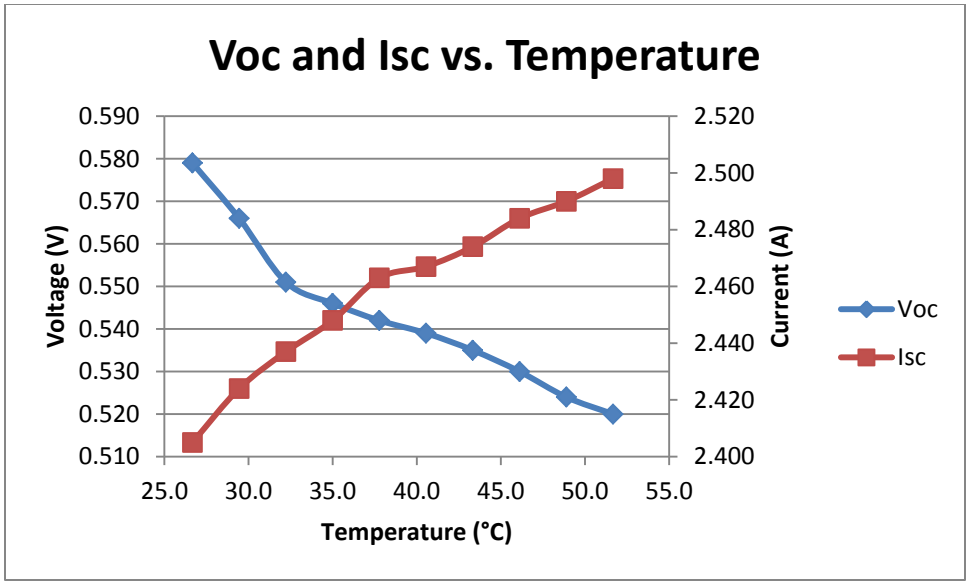

Figure 4-11. V_{OC} and I_{SC} as Functions of Temperature (°C)

The temperature range over which the solar cell was tested is 26.7-51.7 °C (80-125 °F), with incremental changes of 2.8 °C (5 °F). (This test was conducted by direct application of radiant heat energy to the solar cell.) As expected, the open-circuit voltage decreases and the short-circuit current increases as the temperature rises.

The area of the solar array that is necessary to produce enough power to run the electrolyzer stack postulated in Chapter 3 using the solar cell under test in this work is calculated in equations 4-14 to 4-16.

$$A_{array} = A_{solar} \times \frac{E_{e\_stack}^{in}}{P_{solar,max} \times t_{noon}} \tag{4-14}$$

$$A_{array} = 116.13\ cm^2 \times \frac{34.1\ kWh}{0.893\ W \times 8\ hr} \tag{4-15}$$

$$A_{array} = 55.5\ m^2 = 597\ ft^2 \tag{4-16}$$

According to the National Association of Home Builders, a 2009 survey of 54 home builders states that the average home size was slightly greater than 2700 square feet [15]. Consequently, this solar array would fit comfortably on the roof of the average U.S. home represented in the survey (assuming a footprint greater than 600 square feet).

CHAPTER 5: CONCLUSION

The scaled up versions of the electrolyzer, fuel cell and the solar array (based on the solar cell utilized in this study) presented no technical problems with regard to power or spacing constraints. Notwithstanding, the system would work best in cool, sunny environments. The amount of hydrogen equivalent to 32 kWh of fuel is calculated in equation 5-1.

$$32\ kWh \times \frac{3.6\ MJ}{1\ kWh} \times \frac{1\ kg\ H_2}{141.86\ MJ} = 0.812\ kg\ H_2 \tag{5-1}$$

The volume of this amount of hydrogen gas is approximated using the ideal gas law [9] as shown in equations 5-2 and 5-3.

$$V = \frac{n \times R \times T}{P} = \frac{\left(0.812\ kg\ H_2 \times \frac{1\ mol\ H_2}{2.01595\ g\ H_2}\right) \times 8.31451\ \frac{atm \times mL}{mol \times °K} \times 297.04\ °K}{1\ atm} \tag{5-2}$$

$$V = 9{,}818{,}559\ mL = 9819\ L = 2594\ gal \tag{5-3}$$

This volume represents a relatively large tank at atmospheric pressure. Since it is more likely for the hydrogen to be stored at pressures greater than one atmosphere, the size of the storage tank may be reduced significantly. However, the added need for a compressor would increase the total energy consumption of the system. Furthermore, because the back-up power system generates dc output, additional power conditioning equipment such as an inverter may be necessary if the end use requires ac power.

Assuming a tank volume of 40 gallons, the amount of energy required to pressurize the hydrogen at an ambient temperature of 23.9 °C (75 °F) is calculated in equations 5-4 and 5-5.

$$P = \frac{n \times R \times T}{V} = \frac{\left(0.812\ kg\ H_2 \times \frac{1\ mol\ H_2}{2.01595\ g\ H_2}\right) \times 8.31451\ \frac{atm \times mL}{mol \times °K} \times 297.04\ °K}{151{,}416.5\ mL} = 65\ atm \quad (5\text{-}4)$$

$$E_{H2} = P \times V = 65\ atm \times 151{,}416.5\ mL = 0.28\ kWh \quad (5\text{-}5)$$

Utilizing a compressor of 70% efficiency (typical of the rotary type) would increase the overall system energy requirement by approximately 0.40 kWh. This amount of energy is equivalent to an additional 10.2 g H_2 that must be generated.

CHAPTER 6: FURTHER RESEARCH

Further investigation will be necessary to gain more insight into the feasibility of a hydrogen based residential back-up power system. The hope is that through the analysis of more and different data, greater power densities and higher operating efficiencies may be achieved. The modular construction of the system lends itself well to the optimization of individual components. For the solar array, additional research could include solar energy concentration, sun tracking hardware, and the use of novel substrate materials. Fuel cell research could incorporate operation at higher pressures (> 1 atm), use of pure oxygen (as opposed to ambient air), and more efficient water management. Finally, electrolyzer research could integrate new data regarding higher operating pressures (>1 atm) and the use of better materials for the catalyst and membrane electrode assembly.

REFERENCES

[1] J. Duncan Glover, Mulukutla S. Sarma, and Thomas J. Overbye. *Power System Analysis and Design*, 4th edition: 2. Stamford, CT: Cengage Learning, 2008. Print.

[2] "*How much electricity does an American Home Use?*" EIA, 2011. Web. 27 Jan. 2013. < http://www.eia.gov/tools/faqs/faq.cfm?id=97&t=3>

[3] Xiao-Zi Yuan, Chaojie Song, Haijiang Wang, and Juijun Zhang. Electrochemical Impedance Spectroscopy in PEM Fuel Cells: Fundamental and Applications, 1st edition: 2. London: Springer, 2010. Print.

[4] Xiao-Zi Yuan, Chaojie Song, Haijiang Wang, and Juijun Zhang. Electrochemical Impedance Spectroscopy in PEM Fuel Cells: Fundamental and Applications, 1st edition: 13. London: Springer, 2010. Print.

[5] "Standard Reduction Potentials." Jesuit New Orleans AMDG, 2011. Web. 3 Mar. 2013. <http://www.jesuitnola.org/upload/clark/refs/red_pot.htm>

[6] David Sadava, H. Craig Heller, Gordon H. Orians, et al. Life: The Science of Biology, 8th edition: 34. Sunderland, MA: Sinauer Associates Inc., 2008. Print.

[7] "*Dupont Fuel Cells: DuPont Nafion PFSA Membranes.*" DuPont, 2009. Web. 4 Oct. 2012. <http://www2.dupont.com/FuelCells/en_US/assets/downloads/dfc101.pdf>

[8] "*PEM Electrolyzers.*" Horizon Fuel Cell Technologies, 2007. Web. 4 Oct. 2012. <http://www.horizonfuelcell.com/store/peme.htm>

[9] William L. Masterton, Cecile N. Hurley. Chemistry: Principles and Reactions, 6th edition, 107. Belmont, CA: Brooks/Cole Cengage Learning, 2009. Print.

[10] "*Three Photovoltaic Technologies: Monocrystalline, Polycrystalline and Thin Film.*" Wholesale Solar, 2011. Web. 4 Oct. 2012. <http://www.wholesalesolar.com/Information-SolarFolder/celltypes.html>

[11] (2012). "*Effect of Parasitic Resistance.*" Photovoltaic Education Network, n.d. Web. 4 Oct. 2012. <http://www.pveducation.org/pvcdrom/solar-cell-operation/effect-of-parasitic-resistances>

[12] Martin Wolf and Hans Rauschenbach. “Series Resistance Effects on Solar Cell Measurements.” *Advanced Energy Conversion,* vol. 3 1963: 455-479. Pergamon Press

[13] Theodore F. Bogart Jr., Jeffrey S. Beasley, and Guillermo Rico. *Electronic Devices and Circuits*, 6th edition: 12-13. Upper Saddle River: Pearson, 2004. Print.

[14] Theodore F. Bogart Jr., Jeffrey S. Beasley, and Guillermo Rico. *Electronic Devices and Circuits*, 6th edition: 18. Upper Saddle River: Pearson, 2004. Print.

[15] “*Breaking Down House Price and Construction Costs.*” National Association of Home Builders, 2010. Web. 27, Jan. 2013. < http://www.nahb.org/fileUpload_details.aspx?contentID=85253&fromGSA=1>

APPENDIX A: DETERMINATION OF IRRADIANCE

The light source used to illuminate the solar cell under test in this work was a 1500 lumens/100 W halogen floodlight. In order to calculate the irradiance of the incident light striking the surface of the solar cell, it was first necessary to determine the bulb's output power. The equipment used to accomplish this task was the following: a halogen flood light, a flat circular aluminum pan (painted black) filled with water, a thermometer, and a stop watch. To begin the process, the water volume was measured. The mass to volume ratio of water is close to one; therefore, the volume in milliliters is numerically equal to the mass in grams. After measuring the diameter of the aluminum container, the surface area of the water was calculated in equation A-1.

$$A_{H2O} = \pi \times \left(\frac{D}{2}\right)^2 = \pi \times \left(\frac{17.46\ cm}{2}\right)^2 = 239.5\ cm^2 \qquad \text{(A-1)}$$

The following definitions apply in equation A-1:

$A_{H2O} =$ Area of water surface, and

$D =$ Diameter of water surface.

Subsequent to allowing the water temperature to reach equilibrium with that of the ambient air, the light source was placed a distance of 10.16 cm (4 in) away from it. This initial temperature was measured and recorded. Next, the light source was switched on while the timer was simultaneously started. After permitting the water temperature to rise for a total of 15 minutes, the timer was stopped and the light source switched off. The new water temperature was immediately measured and recorded. This process was repeated six more times for incremental

increases in distance of 10.16 cm (4 in). Thus, the light energy, power, and irradiance over the water surface at each distance were determined according to equations A-2 through A-4.

$$E_{H2O} = m_{H2O} \times (T_F - T_I) \times S_{H2O} \quad \text{(A-2)}$$

$$P_{H2O} = \frac{E_{H2O}}{\Delta t} \quad \text{(A-3)}$$

$$Irr = \frac{P_{H2O}}{A_{H2O}} \quad \text{(A-4)}$$

The following definitions apply in equations A-2 to A-4:

$E_{H2O} =$ Energy aborbed by water (J),

$m_{H2O} =$ Mass of water (g),

$T_F =$ Final measured tempetature(°C),

$T_I =$ Initial measured tempetature(°C),

$S_{H2O} =$ Specific heat of water, accepted value $\left(4.187 \frac{\text{J}}{\text{°C}\times\text{g}}\right)$,

$P_{H2O} =$ Output power from light source over water surface (W),

$\Delta t =$ Elapsed time between temperature measurements (s),

$Irr =$ Irradiance of light source over water surface, and

$A_{H2O} =$ Area of water surface.

The results are show in Table A-1.

Distance (cm)	Ti (°C)	Tf (°C)	Δt	E_H_2O (J)	P_H_2O (W)	Irr_H_2O (W / cm^2)
10.16	24.4	37.2	12.8	25315.2	28.13	0.1174
20.32	24.4	35.6	11.1	22013.2	24.46	0.1021
30.48	24.4	32.8	8.3	16509.9	18.34	0.0766
40.64	24.4	30.6	6.1	12107.3	13.45	0.0562
50.8	23.3	28.3	5.0	9905.9	11.01	0.0460
60.96	24.4	28.3	3.9	7704.6	8.56	0.0357
71.12	24.4	26.7	2.2	4402.6	4.89	0.0204

Table A-1. Light Energy, Power, and Irradiance

In order to evaluate the percent error, the thermometer was used to measure both the freezing point and boiling point of water at an atmospheric pressure of 30.11 inHg. The freezing point of water was measured as 1.1 °C (34 °F); the boiling point was measured as 99.4 °C (211 °F). Assuming the error to be linear with respect to the temperature gives a slope as found in equation A-5.

$$m = \frac{T_B - T_Z}{e_B - e_Z} = \frac{99.4\,^{\circ}\mathrm{C} - 1.1\,^{\circ}\mathrm{C}}{(-0.6)^{\circ}\mathrm{C} - 1.1^{\circ}\mathrm{C}} = -59 \qquad \text{(A-5)}$$

The following definitions apply in equation A-5:

$m =$ error slope,

$T_B =$ Measured boiling point of water,

$T_Z =$ Measured freezing point of water,

$e_B =$ Difference between measure and accepted values (boil @ 100 °C), and

$e_Z =$ Difference between measure and accepted values (freeze @ 0 °C).

Using the calculated error slope, the correction factors for the initial and final measured water temperatures may be found according to equations A-6 and A-7.

$$e_I = \frac{T_I - T_Z}{m} + e_Z \qquad \text{(A-6)}$$

$$e_F = \frac{T_F - T_Z}{m} + e_Z \quad \text{(A-7)}$$

The results for equations A-6 and A-7 are presented in Table A-2.

Ti (°C)	Tf (°C)	e_b (°C)	e_z (°C)	e_i (°C)	e_f (°C)
24.4	37.2	-0.6	1.1	0.7	0.5
24.4	35.6	-0.6	1.1	0.7	0.5
24.4	32.8	-0.6	1.1	0.7	0.6
24.4	30.6	-0.6	1.1	0.7	0.6
23.3	28.3	-0.6	1.1	0.7	0.6
24.4	28.3	-0.6	1.1	0.7	0.6
24.4	26.7	-0.6	1.1	0.7	0.7

Table A-2. Error Calculations

Now, the new light energy, from which power and irradiance are found, can be calculated according to equation A-8.

$$E_{H2O} = m_{H2O} \times \{(T_F - e_F) - (T_I - e_I)\} \times S_{H2O} \quad \text{(A-8)}$$

Of course, the power and irradiance may be found using equations A-3 and A-4. Finally, the percent error can be calculated in accordance with equation A-9.

$$\%error = 100\% \times \frac{Measured - Theortical}{Theortical} \quad \text{(A-9)}$$

The results for the newly calculated light energy, power, irradiance, and percent error are all shown in Table A-3.

Distance (cm)	Ti (°C)	Tf (°C)	E_H_2O (J)	P_H_2O (W)	Irr_H_2O (W / cm^2)	% error
10.16	24.4	37.2	25744.3	28.60	0.1194	-1.7
20.32	24.4	35.6	22386.3	24.87	0.1039	-1.7
30.48	24.4	32.8	16789.7	18.66	0.0779	-1.7
40.64	24.4	30.6	12312.5	13.68	0.0571	-1.7
50.8	23.3	28.3	10073.8	11.19	0.0467	-1.7
60.96	24.4	28.3	7835.2	8.71	0.0364	-1.7
71.12	24.4	26.7	4477.3	4.97	0.0208	-1.7

Table A-3. Adjusted Light Energy, Power, Irradiance, and Percent Error

These small errors are negligible.

APPENDIX B: MATLAB CODE FOR SIMULATIONS

```
% Solar cell simulation plots from Chapter 4
clc
clear all
close all

Is = 1e-6;                    % Diode Reverse Current
q = 1.60217733e-19;           % Electron Charge
eta = 1.583722347911;         % Diode Emission Coefficient
k = 1.380658e-23;             % Boltzmann Constant
Tf = 85;                      % Fahrenheit Temperature
T = (5/9) * (Tf + 459.67);    % Kelvin Temperature
Vt = (k * T) / q;             % Thermal Voltage in Volts
Ig = 0.6;                     % Light-Generated Current in Amps
VL = zeros(1,1001);           % Load Voltage Vector (Volts)
IL = zeros(1,1001);           % Load Current Vector (Amps)

% Vary Light-Generated Current (Figure 4-6)
Rs = 0.167;
Rsh = 211.573;
color = ['b', 'g', 'r', 'c','m','y','k'];
hold on
for n = 1:6
    num = 1;
    for RL = 0:0.05:50
        VD = solve('Ig = Is*(exp(VD/(eta*Vt))-1) + VD/Rsh + VD/(Rs+RL)',
'VD');
        IL(num) = subs(VD) / (Rs + RL);
        VL(num) = subs(VD) - IL(num) * Rs;
        num = num + 1;
    end
    plot(VL,IL,color(n), 'LineWidth', 2)
    Ig = Ig + 0.6;
end
legend('I_G = 0.6 A', 'I_G = 1.2 A', 'I_G = 1.8 A', 'I_G = 2.4 A', 'I_G = 3
A', 'I_G = 3.6 A')
xlabel('Load Voltage (V)')
ylabel('Load Current (A)')
title('Varying Light Generated Current')
hold off

Ig = 2;
% Vary Shunt Resistance (Figure 4-4)
figure
Rs = 0.167;
Rsh = 211.573;
color = ['b', 'g', 'r', 'm'];
```

```
hold on
for n = 1:4
    num = 1;
    for RL = 0:0.05:50
        VD = solve('Ig = Is*(exp(VD/(eta*Vt))-1) + VD/Rsh + VD/(Rs+RL)',
'VD');
        IL(num) = subs(VD) / (Rs + RL);
        VL(num) = subs(VD) - IL(num) * Rs;
        num = num + 1;
    end
    plot(VL,IL,color(n), 'LineWidth', 2)
    Rsh = Rsh / 10;
end
legend('Rsh = 211 ohms', 'Rsh = 21.1 ohms', 'Rsh = 2.11 ohms', 'Rsh = 0.211
ohms')
xlabel('Load Voltage (V)')
ylabel('Load Current (A)')
title('Varying Shunt Resistance')
hold off

% Vary Series Resistance (Figure 4-5)
figure
Rsh = 211.573;
hold on
for n = 1:4
    num = 1;
    for RL = 0:0.05:50
        VD = solve('Ig = Is*(exp(VD/(eta*Vt))-1) + VD/Rsh + VD/(Rs+RL)',
'VD');
        IL(num) = subs(VD) / (Rs + RL);
        VL(num) = subs(VD) - IL(num) * Rs;
        num = num + 1;
    end
    plot(VL,IL,color(n), 'LineWidth', 2)
    Rs = Rs * 2;
end
legend('Rs = 0.167 ohms', 'Rs = 0.334 ohms', 'Rs = 0.668 ohms', 'Rs = 1.336
ohms')
xlabel('Load Voltage (V)')
ylabel('Load Current (A)')
title('Varying Series Resistance')
hold off
```